Dynamic entropy as a measure of caging and persistent particle motion in supercooled liquids

Paolo Allegrini, Jack F. Douglas,* and Sharon C. Glotzer*
Polymers Division and Center for Theoretical and Computational Materials Science, National Institute of Standards and Technology, Gaithersburg, Maryland, 20899
(Received 18 December 1998)

The length-scale dependence of the dynamic entropy is studied in a molecular dynamics simulation of a binary Lennard-Jones liquid above the mode-coupling critical temperature T_c. A number of methods exist for estimating the entropy of dynamical systems, and we utilize an approximation based on calculating the mean first-passage time (MFPT) for particle displacement because of its tractability and its accessibility in real and simulation measurements. The MFPT dynamic entropy $S(\epsilon)$ is defined as equal to the inverse of the average first-passage time for a particle to exit a sphere of radius ϵ. This measure of the degree of chaotic motion allows us to identify characteristic time and space scales and to quantify the increasingly correlated particle motion and intermittency occurring in supercooled liquids. In particular, we identify a ''cage'' size defining the scale at which the particles are transiently localized, and we observe persistent particle motion at intermediate length scales beyond the scale where caging occurs. Furthermore, we find that the dynamic entropy at the scale of one interparticle spacing extrapolates to zero as the mode-coupling temperature T_c is approached.
[S1063-651X(99)00711-4]

PACS number(s): 61.20.Lc, 02.70.Ns, 05.60.−k, 05.45.Gg

I. INTRODUCTION

It has been suggested that the glass transition in cooled liquids is a dynamic transition from an ergodic to a nonergodic state. For example, the ideal mode-coupling theory predicts that the molecules of simple liquids become increasingly ''caged'' by surrounding molecules, resulting in an ergodic to nonergodic transition at a critical temperature T_c at which the fluid molecules become permanently localized (i.e., the self-diffusion coefficient vanishes) [1]. Although a tendency toward particle localization for increasingly long times has been observed in simulations and experiments on supercooled liquids, particle localization and structural arrest does not actually occur at the extrapolated temperature T_c because the particles are eventually able to ''escape'' their cages. Recent simulations have also shown the tendency for particle motion to occur in an increasingly correlated way in supercooled liquids [2–8], a feature emphasized by the older, phenomenological Adam-Gibbs model of glass formation [9]. The observed greater particle mobility near T_c is presumably a consequence of the increased collective motion of cooled liquids (''hopping'' in the extended version of the mode-coupling theory [1]) which restores the ergodicity of the liquid for some temperature range below T_c. This thermally activated collective motion apparently postpones the ergodic to nonergodic transition to a lower temperature. In the Adam-Gibbs model [9], this lower temperature corresponds to the conjectured ''ideal'' glass transition temperature T_0, where the equilibrium configurational entropy extrapolates to zero [10].

If glass formation indeed represents an ergodic to nonergodic dynamic transition, then it is important to define a dynamical measure of order that quantifies both the ''closeness'' of the transition [11] and the degree of correlated motion in an equilibrium glass-forming liquid. Ergodic theory provides us with a natural measure in the form of the ''dynamic entropy'' [12–17].

The concept of dynamic entropy was introduced by Shannon in his theory describing the capacity of ideal communication devices to transmit information [18]. This idea was later developed by Kolmogorov and others [13] into a general measure of the ''degree of randomness'' or ''degree of chaos'' of dynamical systems. According to Pessin's theorem [19], the Kolmogorov-Sinai dynamic entropy h_{KS} for a Hamiltonian dynamical system equals the sum of the positive Lyapunov exponents [19,20]. These exponents are measures of the ''instability'' of the system evolution [12,16]. Dynamic entropy extends the equilibrium definition of entropy from statistical mechanics to the *time domain*. The dynamical entropy provides an estimate of the rate of growth of ''information'' (per unit time) required to describe the evolution of a dynamical system [14,15,21], and is also a measure of the ''complexity'' of a dynamical system [22]. The dynamic entropy characteristically decreases as a system orders and its exploration of its phase space becomes more restricted [23,24]. Thus, the dynamic entropy decreases as a fluid crystallizes or a magnet orders [24–27].

The Kolmogorov-Sinai dynamic entropy has some shortcomings in the description of complex configurational changes that occur in supercooled liquids. In particular, h_{KS} diverges for the ideal process of Brownian motion (due to the nondifferentiability of the trajectories) [14,28,29]. Consequently, we must anticipate difficulties in applying dynamic entropy to quantify particle motions at large length and time scales in the case of supercooled liquids. Recently, there has been an important generalization of the dynamic entropy concept that provides a ''bridge'' between microscopic dynamical system descriptions and macroscopic stochastic descriptions of liquid dynamics. This generalization

*Authors to whom correspondence should be addressed. Electronic addresses: sharon.glotzer@nist.gov and jack.douglas@nist.gov

recognizes that the amount of information required to describe the paths of a stochastic process depends strongly on the length scale of observation ϵ. The ϵ-dependent dynamic entropy $h(\epsilon)$ of Gaspard and Wang and others [14] (also called ''ϵ entropy'') reduces to the h_{KS} entropy in the limit of small ϵ,

$$\lim_{\epsilon \to 0} h(\epsilon) = h_{\mathrm{KS}}, \tag{1.1}$$

and is well defined for idealized stochastic processes at a fixed, nonvanishing ϵ. The dynamic entropy of a Brownian particle $h_B(\epsilon)$ obeys the scaling relation,

$$h_B(\epsilon) \propto \epsilon^{-2}, \quad \epsilon > 0, \tag{1.2}$$

where the proportionality constant is fixed by the particle diffusion coefficient [14]. As mentioned above, $h(\epsilon)$ for stochastic particle motion diverges as $\epsilon \to 0$, and the exponent reflects the fractal dimension of the particle trajectories [14,30]. Specifically, the exponent 2 in Eq. (1.2) is the Hausdorff dimension of a Brownian path in three dimensions [31], and in the limit of perfectly coherent (ballistic) particle motion this exponent is 1. In idealized stochastic processes (e.g., fractional Brownian motion, Lévy flights, etc.) the exponent in Eq. (1.2) can be identified with the path Hausdorff dimension [13,14,30,32], and can take values intermediate between 1 and 2. This exponent reflects the ''degree of persistence'' in the particle displacement relative to Brownian motion.

The scale dependent dynamic entropy $h(\epsilon)$ for complex dynamical systems such as liquids depends strongly on the observational scale ϵ. At very small ϵ the microscopic chaotic motion of the molecules is observed, so that $h(\epsilon)$ varies slowly with ϵ. The decorrelation of particle velocities in a liquid occurs at a time and space scale corresponding to the average interparticle ''collision time,'' and $h(\epsilon)$ starts varying with ϵ as this decorrelation occurs. This helps us to identify a characteristic space and time scale over which the bare microscopic dynamics can be coarse grained by a stochastic description. Correlations associated with particle displacement arise at longer times in cooled liquids, and $h(\epsilon)$ also helps us in determining the spatial and time scales over which these correlations occur. $h(\epsilon)$ thus provides a measure of the degree of chaotic motion appropriate to the description of real systems at arbitrary observational scales, and is an attractive tool for quantifying the increasingly correlated motion in cooled liquids. It is notable that its definition is not restricted to circumstances where statistical mechanical equilibrium exists, so that this measure of the degree of chaos extends to nonequilibrium situations such as the glass state and turbulent fluids [14].

The calculation of $h(\epsilon)$ [14] (or h_{KS}) is generally difficult, especially in cases where h_{KS} is small and long computational times are required for its accurate determination [14,25]. In the present paper, we utilize a simple approximation for $h(\epsilon)$ that has the advantage of being accessible in experiments on real materials and computer simulations [14,33]. Provided that the spatial scale ϵ is not too small [14], $h(\epsilon)$ can be approximated by enclosing the particle position at time $t=0$ by a sphere of radius ϵ centered on the particle, and then determining the time τ at which the trajectory first arrives at the threshold distance ϵ (see Fig. 1). We average this ''first-passage time'' over all particles in the liquid to obtain the mean first-passage time (MFPT) $\tau(\epsilon)$, and we define the ''MFPT dynamic entropy'' $S(\epsilon)$ as

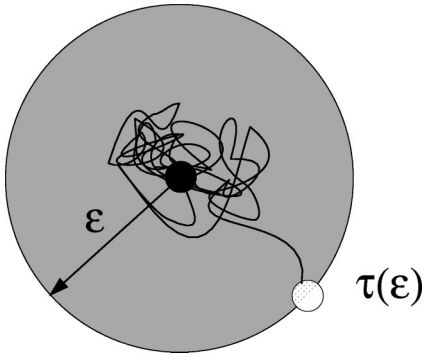

FIG. 1. Schematic of a particle trajectory in a cooled liquid. The gray region represents the ϵ sphere. $\tau(\epsilon)$ is the first-passage time for the particle to reach the boundary of the ϵ sphere. The filled circle denotes the initial particle position, and the open circle denotes the particle at the first-passage time.

$$S(\epsilon) \equiv 1/\tau(\epsilon), \tag{1.3}$$

where

$$\tau(\epsilon) \equiv \int_0^\infty dt\ P_\epsilon(t)\ t. \tag{1.4}$$

$P_\epsilon(t)dt$ is the probability that the particle reaches the distance ϵ between t and $t+dt$. The dynamic entropy $S(\epsilon)$ is thus one measure of the average ''escape rate'' of a particle from its local environment [34]. We note that although the definition of $S(\epsilon)$ is motivated by dynamical systems theory concepts, this property defines an independently interesting measure of correlated motion in liquids that does not rely on the approximation relating $S(\epsilon)$ to $h(\epsilon)$.

In this paper we utilize $S(\epsilon)$ to identify characteristic space and time scales in the particle dynamics, and to quantify the increasingly correlated motion observed in previous analyses of the same simulations considered in the present paper. These studies indicated the development of large scale dynamical heterogeneity and the nature of this dynamical heterogeneity has been examined in a series of recent papers that are complementary to the present work [2–7]. There it was established that transient clusters of highly ''mobile'' particles form in the cooled liquid, and that the average size of these clusters grows rapidly as T_c is approached [3]. A pair distribution function for particle displacements was defined, and this quantity exhibits a growing length scale upon cooling that reflects the clustering of mobile particles [5–7]. The growing length scale is time dependent, and attains a peak value at a time in the α-relaxation regime [6,7].

It has also been shown in the present liquid that the particles within the mobile particle clusters move in cooperatively rearranging ''strings'' [2,35]. Notably, the stringlike collective motion also begins well above T_c, but the strings themselves exhibit no tendency to grow rapidly near T_c. Instead, the length distribution of the strings is found to be nearly exponential, and a similarity of this distribution to that

commonly observed in equilibrium polymerization has been noted [2]. Donati *et al.* [2] suggested that the growing barrier height to particle motion is proportional to the average string length, which would imply that these stringlike motions have a basic significance for understanding transport in cooled liquids. Thus stringlike correlated particle motion appears to be an important mode of motion in our cooled liquid [2] and part of the motivation of the present work is to better characterize the development of this type of collective motion. We are also interested in the extent to which particle displacement becomes intermittent in time in cooled liquids, since a growing intermittency in particle motion has been suggested to underlie the glass transition [36,37].

The paper is outlined as follows. In Sec. II we review some details of the molecular dynamics simulation data utilized in this work. Section III examines $S(\epsilon)$ over a broad range of scales, and dynamical regimes are defined where the motion is ballistic, transiently localized, persistent, and diffusive. These regimes are examined in separate subsections. We summarize our findings in Sec. IV.

II. SIMULATION DETAILS

The system studied is a three-dimensional binary mixture of 8000 Lennard-Jones (LJ) particles in which the sizes of the particles and the interaction parameters are chosen to prevent crystallization and demixing [38]. The size of the A particles is about 10% larger than that of the B particles (while the mass is the same), and the particles have a relative concentration 80:20 of A particles to B particles. We report our results in dimensionless LJ units [38]. The system was equilibrated at different temperatures T in the range 0.451–0.550. The density ρ varied from 1.09 particles per unit volume at the highest temperature to 1.19 at the lowest T simulated. For reference, the mode-coupling temperature T_c for this system is $T_c=0.435$ at $\rho\simeq 1.20$ [2,7,39], so all the simulation data analyzed here are well above the glass transition. Configurational histories for up to 4×10^6 molecular dynamics time-steps following equilibration were stored for each run. Following equilibration in the *NPT* and *NVT* ensembles, the trajectories were calculated in an *NVE* ensemble, and snapshots containing the particle coordinates and velocities were taken at logarithmic time intervals during the run. Here N, P, V, T, and E denote constant particle number, pressure, volume, temperature, and energy, respectively. In this stage, the equations of motion were integrated using the velocity Verlet algorithm with a step size of 0.0015 at the highest temperature, and 0.003 at all other temperatures. Adopting argon values for the LJ parameters of the large particles implies an observation time of ≈ 26 ns for the coldest T. All data presented here are calculated for the majority (A) particles only, except where otherwise noted [40]. Further details of the simulation can be found in Ref. [3].

Over the temperature-density regime studied, the system exhibits the usual features of a fragile [41], glass-forming liquid. For example, the mean square displacement $\langle r^2(t)\rangle \equiv \langle (1/N_A)\,\Sigma_{i=1}^{N_A}|\mathbf{r}_i(t)-\mathbf{r}_i(0)|^2\rangle$ for the A particles is shown in Fig. 2 for different T. Here $\mathbf{r}_i(t)$ is the position of particle i at time t, N_A is the number of A particles (6400), and $\langle\cdots\rangle$ denotes an ensemble average. For each state point, a ''plateau'' exists in both the mean square displacement and the self-part of the intermediate scattering function $F_s(\mathbf{q},t)$ as a function of t. The plateau in Fig. 2 separates an early time ''ballistic'' regime from a late time diffusive regime. The plateau is interpreted as implying ''caging'' of the particles, and this phenomenon is typical for liquids at low temperature or high density. Over the range of T studied, the α-relaxation time τ_α, describing the decay of $F_s(\mathbf{q},t)$ (at the value of q corresponding to the first peak in the static structure factor), increases by 2.4 orders of magnitude, and follows a power law $\tau_\alpha \sim (T-T_c)^{-\gamma}$, with $T_c\simeq 0.435$ and $\gamma\simeq 2.8$. The simulated liquid states analyzed here therefore exhibit relaxation behavior characteristic of a supercooled liquid. No long range structural correlations due to density or composition fluctuations are apparent in the simulation data [3].

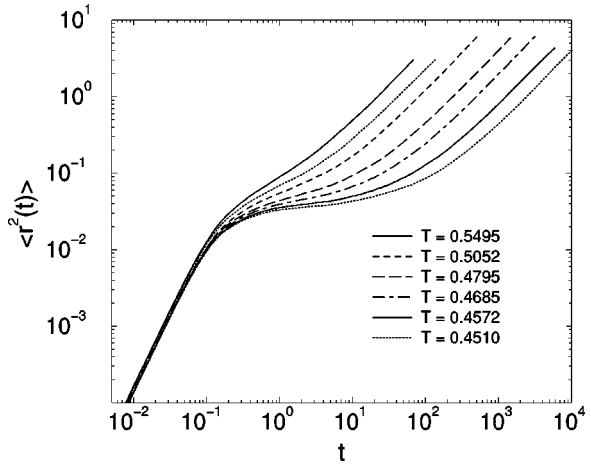

FIG. 2. Mean square displacement of the majority species (A particles) vs time for different T.

III. CHARACTERISTIC DECORRELATION TIME AND SPACE SCALES

In Fig. 3 we show the MFPT $\tau(\epsilon)$ versus ϵ for six differ-

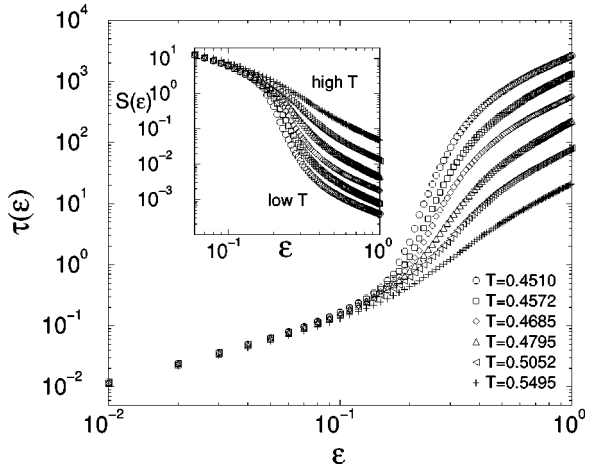

FIG. 3. Mean first-passage time τ of the majority species (A particles) vs ϵ, for different T. Inset: Mean first-passage time dynamic entropy $S(\epsilon)$. Compare the $S(\epsilon)$ variation observed here for a cooled liquid with the dynamic entropy $h(\epsilon)$ calculated for a one-dimensional model map exhibiting diffusion at long times [compare the present figure with Fig. 25(b) of Gaspard and Wang [8]].

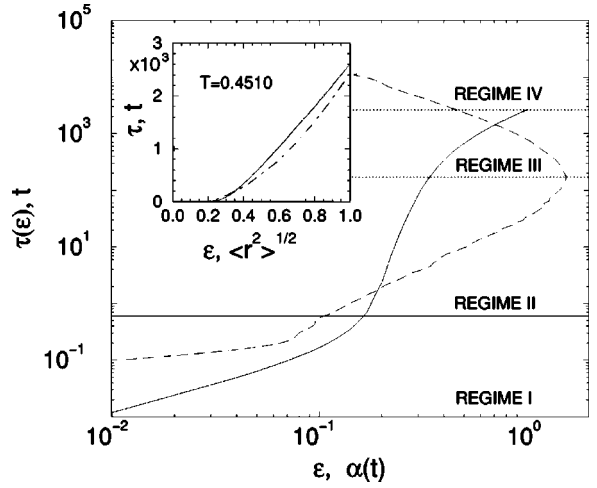

FIG. 4. Classification of dynamic regimes. MFPT $\tau(\epsilon)$ (solid curve) plotted vs ϵ, and the non-Gaussian parameter $\alpha(t)$ (dashed curve) plotted vs t, for $T=0.451$. Inset: Comparison between $\tau(\epsilon)$ (solid curve) and $\langle r^2(t)\rangle$ (dot-dashed curve) on a linear scale.

ent runs corresponding to varying the temperature of the system from $T=0.550$ to 0.451. In the inset we show the dynamic entropy $S(\epsilon)\equiv 1/\tau(\epsilon)$. Note that the variation of $\tau(\epsilon)$ with ϵ exhibits similar qualitative trends to the variation of t with $\langle r^2(t)\rangle$ shown in Fig. 2.

For small ϵ, corresponding to the inertial regime, $S(\epsilon)$ is insensitive to temperature. At intermediate ϵ values we see a decrease of $S(\epsilon)$ with decreasing T and an increase in the magnitude of the slope in the log-log plot. A strong temperature dependence of $S(\epsilon)$ is apparent at a scale on the order of one interparticle distance ($\epsilon=1$). On these larger scales, we show in a later subsection that $S(\epsilon)$ exhibits a power-law scaling with ϵ and reduced temperature.

It is apparent from Fig. 2 that the particle displacement in this cooled liquid is not Brownian over most of the simulation time scales, and it is conventional to quantify this deviation by a ''non-Gaussian parameter'' $\alpha(t)$ involving the moments $\langle r^2(t)\rangle$ and $\langle r^4(t)\rangle$ of the self-part of the van Hove correlation function $G_s(r,t)\equiv\langle(1/N_A)\sum_{i=1}^{N_A}\delta[\mathbf{r}-(\mathbf{r}_i(t)-\mathbf{r}_i(0))]\rangle$. The parameter $\alpha(t)$ is defined as

$$\alpha(t)\equiv\frac{3\langle r^4(t)\rangle}{5\langle r^2(t)\rangle^2}-1, \tag{3.1}$$

and vanishes for Brownian motion. $\alpha(t)$ is shown in Fig. 4 together with $\tau(\epsilon)$ for the coldest run ($T=0.451$); note that for $\alpha(t)$, time t is plotted on the ordinate axis. This comparison allows us to identify four regimes: an inertial regime (regime I) where the non-Gaussian parameter is small; a ''localization'' regime characterized by a large value for the slope in the $\tau(\epsilon)$ log-log plot and by a growing $\alpha(t)$ (regime II); a regime of particle motion that is persistent relative to Brownian motion, and where $\alpha(t)$ decreases (regime III); and a fourth regime where the non-Gaussian parameter has decayed back to very small values so that the particle motion is nearly Brownian (regime IV). The four regimes are examinated in detail in the following subsections.

We emphasize that while some parallelism exists between the mean square displacement and the first-passage time, the inset of Fig. 4 comparing these quantities shows that they are not equivalent. However, if the distribution of particle displacments $G_s(r,t)$ were always exactly Gaussian [i.e., $\alpha(t)=0$ for every t], then a simple inverse function relation should hold between these quantities. $G_s(r,t)$ obeys a ''scaling relation'' if we can rescale $G_s(r,t)$ as

$$G_s(r,t)=\frac{1}{t^\nu}f\left(\frac{r}{t^\nu}\right), \tag{3.2}$$

where f is some function. Simple dimensional analysis based on Eq. (3.2) implies,

$$\langle r^2(t)\rangle\propto t^{2\nu}, \tag{3.3}$$

and the scaling of the first-passage time with ϵ,

$$\tau(\epsilon)\propto\epsilon^{1/\nu}. \tag{3.4}$$

In practice, these idealized scaling relations are restricted to certain time and space scales. Scaling with $\nu=1$ is observed in the short time inertial regime. This result can be inferred from the general relation between the second moment of $G_s(r,t)$ and the particle velocity,

$$\langle\dot{\mathbf{r}}(0)\cdot\dot{\mathbf{r}}(t)\rangle=\frac{1}{2}\frac{d^2\langle r^2(t)\rangle}{dt^2}, \tag{3.5}$$

and the constancy of the velocity autocorrelation function at short times [42,43],

$$\langle\dot{\mathbf{r}}(0)\cdot\dot{\mathbf{r}}(t)\rangle\rightarrow\langle\dot{\mathbf{r}}(0)\cdot\dot{\mathbf{r}}(0)\rangle\equiv v_0^2,\quad t\rightarrow 0, \tag{3.6}$$

where v_0 is the average particle velocity. Integrating Eq. (3.5) over a short time interval obviously gives $\langle r^2(t)\rangle\sim t^2$ or ''ballisticlike'' motion. Actually, this scaling is just a consequence of the existence of equilibrium, and should not be construed as necessarily implying the absence of interparticle interactions at short time scales [43]. A Gaussian form for the van Hove correlation function in this short time regime is ensured by the Maxwell-Boltzmann distribution for the particle velocities. In the opposite extreme of very long times, the central limit theorem governing the sum of independent particle displacements implies that the particle displacement distribution is Gaussian, and that $\nu=1/2$. Transient scaling regimes can be observed at intermediate time scales, however. We refer to particle displacements as ''persistent'' relative to Brownian motion if $\nu>1/2$, or ''localized'' relative to Brownian motion if $\nu<1/2$.

A. Inertial regime

In the limit of very small ϵ we probe the fast microscopic dynamics associated with the decorrelation of the particle momenta. It is difficult to probe this decorrelation directly using the first-passage time approximation to the dynamic entropy. Figure 3 indicates that our approximation for the dynamic entropy appears to diverge for $\epsilon\rightarrow 0$, so our approximation must break down in this limit. Gaspard and Wang have pointed out that the first-passage time approximation to the dynamic entropy breaks down in this limit [14], so this shortcoming is to be expected. An estimate of the expected plateau in $S(\epsilon)$ corresponding to the

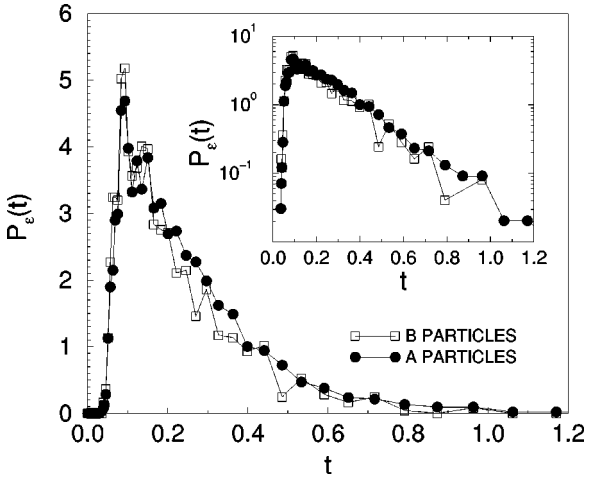

FIG. 5. Probability of first-passage time $P_\epsilon(t)$ for the A and B particles at $T=0.451$ and $\epsilon=0.1$. Inset: Same data represented in a semilog scale.

Kolmogorov-Sinai entropy can be obtained by determining a cutoff time of the first-passage time distributions in the fast dynamics regime.

The dynamics in this regime is examined by setting the magnitude of the first-passage sphere (ϵ sphere) about the center of each particle to be small enough that a collision does not usually occur before the particle leaves the ϵ sphere (see Fig. 1). By focusing on the particle first-passage time in this regime we identify a time and space scale over which particle velocities begin decorrelating. The first-passage time in this regime is insensitive to the type (A or B) of particle, since they have the same mass. This is apparent in Fig. 5, where the first-passage time distributions for both the A and B particles are shown for the coldest run and $\epsilon=0.1$.

The idealization of ballistic particle motion implies the time $\tau(\epsilon)$ it takes for the particle to exit the sphere of radius ϵ equals ϵ/v_0. Figure 6 shows an expanded plot of τ versus ϵ in the small ϵ regime where this linear dependence of τ on

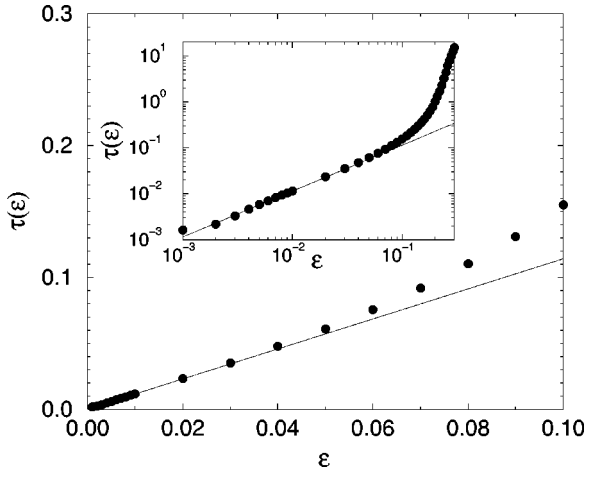

FIG. 6. τ vs ϵ in the small ϵ regime, $0.001<\epsilon<0.15$, for $T=0.468$. Inset: log-log plot of the same data. Note that the asymptotic linear scaling of $\tau(\epsilon)=1.14\epsilon$ (solid lines) breaks down around a value $\epsilon_v\approx0.05$, corresponding to $\tau_v\approx0.6$. ϵ_v and τ_v are approximately independent of temperature (see also Fig. 3). For the T range considered in the simulation.

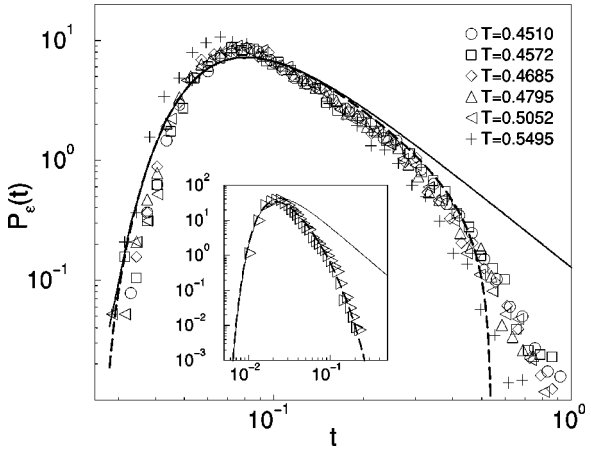

FIG. 7. First-passage time distributions $P_\epsilon(t)$ in the inertial regime. The main figure contains six different temperatures at $\epsilon=0.1$ plotted on a log-log scale. The solid line indicates Eq. (3.7), where the constant of proportionality has been adjusted to best fit the data. The long-dashed line indicates the cutoff distribution function [Eq. (3.8)] with no free parameters. Inset: $P_\epsilon(t)$ at $T=0.468$ for $\epsilon=0.03$. This value of ϵ is less than the velocity decorrelation scale ϵ_v indicated in Fig. 6. Equations (3.7) and (3.8) are also shown in comparison with the simulation data. Note the absence of the long tail in the inset distribution.

ϵ is apparent. A nonlinear dependence of τ on ϵ develops as the particle velocities decorrelate at a ''velocity decorrelation scale'' $\epsilon_v\approx0.05$. This distance corresponds to the time $\tau_v\approx0.6$ (on the order of 10^{-13} s in argon units). We find that ϵ_v and τ_v are approximately independent of temperature in the present simulation (see also Fig. 3).

We obtain further insight into the decorrelation of particle velocities in the inertial regime by examining the distribution of first-passage times, $P_\epsilon(t)$, as a function of ϵ. Figure 7 shows $P_\epsilon(t)$ for $\epsilon=0.1$ and 0.03 for $T=0.468$. We obtain a good approximation to $P_\epsilon(t)$ in the inertial regime through a Gaussian approximation for $G_s(r,t)$ [44] in conjunction with the first-passage distribution for Brownian paths [45]. The first-passage time distribution $P_\epsilon(t)$ scales as

$$P_\epsilon(t)\sim\exp\left(\frac{-\epsilon^2}{2\langle r^2\rangle}\right) \tag{3.7}$$

at short times, and decays exponentially at long times, $P_\epsilon(t)\sim\exp[-t/\tau(\epsilon)]$ [45]. We then introduce the approximation:

$$P_\epsilon\simeq\frac{A}{t^2}\exp\left[-\frac{1}{2}\left(\frac{\epsilon}{v_0t}\right)^2-\frac{t}{\tau(\epsilon)}\right], \tag{3.8}$$

where A is a normalization constant. $\langle r^2\rangle^{1/2}$ in Eq. (3.7) has been replaced by v_0t based on the assumption that the particle displacements are nearly ''ballistic'' in the inertial regime. Note that the limiting expression for $P_\epsilon(t)$ given by Eq. (3.7) can also be deduced by assuming a Maxwell velocity distribution (one dimensional due to the near rectilinear motion) with the velocity replaced by ϵ/t. Figure 7 shows that Eq. (3.7) (solid line) does not provide an accurate fit to the data using $v_0=1/1.14$ from the linear slope in Fig. 6, while the approximate expression Eq. (3.8) fits well for ϵ less

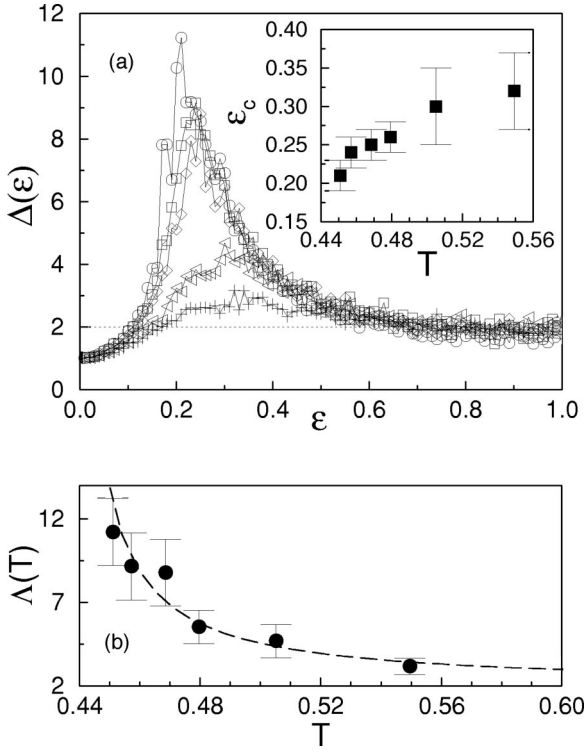

FIG. 8. (a) $\Delta(\epsilon)\equiv d\ln\tau(\epsilon)/d\ln(\epsilon)$ for (from top to bottom) $T=0.451$, 0.457, 0.468, 0.480, 0.505, and 0.550. Inset: ''cage'' size ϵ_c vs T. (b) $\Lambda\equiv\max\Delta(\epsilon)$ plotted vs T. The dashed line is a power-law fit to the data, as indicated in the text.

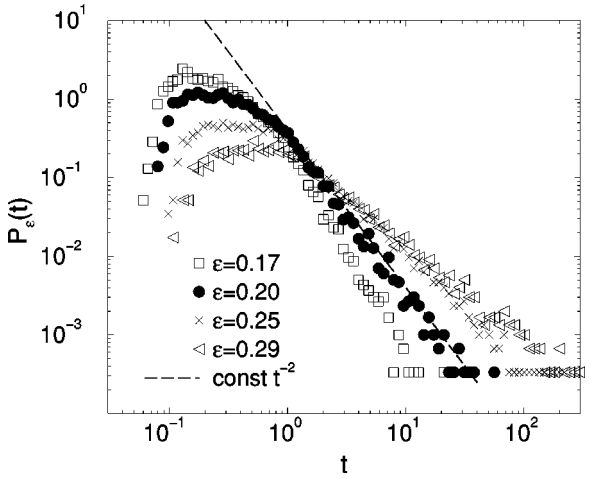

FIG. 9. First-passage time distributions $P_\epsilon(t)$ for $T=0.451$, at different values of ϵ near $\epsilon_c=0.21\pm0.02$. The dashed line indicates an inverse power law t^{-2} for comparison.

than the ''velocity decorrelation scale'' $\epsilon_v\approx0.05$. For $\epsilon>\epsilon_v$, $P_\epsilon(t)$ shows evidence of developing a power-law ''tail'' at long times, as seen in the main part of Fig. 7. This tendency becomes more developed at larger ϵ, as discussed in Sec. III B. The inset of Fig. 7 shows first-passage time data for $\epsilon<\epsilon_v$, where the tail is nearly absent and the cutoff is evident. At this point, we note that in liquids h_{KS} characteristically scales as the inverse of the average interparticle collision time and thus has the interpretation of a microscopic ''collision rate'' [12,14]. The time τ_v can be considered as an average particle collision time, so that an inverse relation between h_{KS} and τ_v is expected. We do not consider the relation between τ_v and h_{KS}, since simulations over a broader temperature range and the direct calculation of the Kolmogorov-Sinai entropy through Lyapunov exponent spectra [46,47] are required for such an investigation.

B. Particle localization regime

The tendency of particle motion to become increasingly localized, as emphasized by the mode-coupling theory, is a conspicuous feature of experimental and simulation data on supercooled liquids. The ''plateau'' in the mean square displacement log-log plots (see Fig. 2) indicates transient particle localization or ''caging,'' and the persistence of this plateau increases with decreasing T [48]. Next we utilize the dynamic entropy concept to quantify this localization.

An increase in the slope of $\ln\tau(\epsilon)$ versus $\ln\epsilon$ in Fig. 3 provides evidence for localization. A numerical differentiation of the data in Fig. 3 is shown in Fig. 8(a), where $\Delta(\epsilon)$ denotes the logarithmic derivative $\Delta(\epsilon)\equiv d\ln\tau/d\ln\epsilon$. The scaling behavior in Eq. (3.4) implies that $\Delta(\epsilon)$ corresponds to the fractal dimension $1/\nu$ of the particle trajectories. Figure 8(a) shows that for all T, $\Delta(\epsilon)\to1$ for small ϵ, and $\Delta(\epsilon)$ seems to approach a constant value $1/\nu$ for large ϵ. At intermediate values of ϵ, we observe that $\Delta(\epsilon)$ develops a maximum at ϵ_c, corresponding to the inflection point in Fig. 3. This length scale defines a distance that is difficult for the particle to exceed, and thus we define ϵ_c as the ''cage'' size. The inset in Fig. 8(a) shows that ϵ_c decreases with temperature, so that increased particle confinement occurs with cooling. Independent evidence indicating the significance of this characteristic scale is discussed later in this subsection.

We denote the value of $\Delta(\epsilon)$ at ϵ_c by the ''localization parameter'' $\Lambda(T)\equiv\max\Delta(\epsilon)=\Delta(\epsilon_c)$, and its T dependence is shown in Fig 8(b). The value of $\Lambda(T)$ increases with cooling, consistent with increasing particle localization ($\nu<1/2$). The relatively noisy data in Fig. 8(b) can be fitted by a power law, $\Lambda(T)=2+0.15(T-T_c)^{-1.03}$, with $T_c=0.435$.

Our identification of the cage size ϵ_c from the maximum value of $\Delta(\epsilon)$ is further supported by the examination of the first-passage time distribution $P_\epsilon(t)$ for ϵ near ϵ_c. We find that $P_\epsilon(t)$ develops a long time power-law tail in this intermediate regime which is symptomatic of the development of intermittency in particle motion and particle localization [36]. In Fig. 9 we show, for $T=0.451$, $P_\epsilon(t)$ at several values of ϵ near $\epsilon_c=0.21\pm0.02$. The apparent power law for the $P_\epsilon(t)$ tail varies with ϵ and has a value near 2 for $\epsilon\approx\epsilon_c$.

This power-law tail behavior in $P_{\epsilon_c}(t)$ is shared by the four coldest temperatures, as shown in Fig. 10, where the asymptotic behavior of the distributions is seen to be numerically very similar. The difference in their first moments [i.e., $\tau(\epsilon_c)$ in Fig. 3] reflects both the differences between the distributions in Fig. 10 at short times, and the asymptotic cutoff in the distributions that is difficult to resolve numerically.

Odagaki [36] suggested that the second and first moments of the first-passage time distribution at the scale of one interparticle distance diverge at T_c and at the glass transition temperature T_g, respectively, and a recent paper by Hiwatari and Muranaka [49] supported this glass transition scenario.

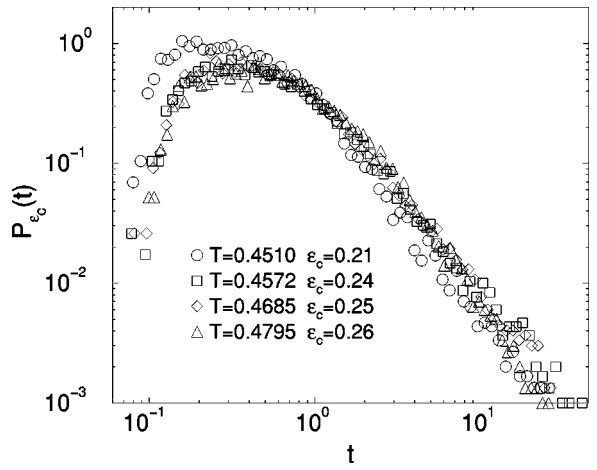

FIG. 10. First-passage time distributions $P_{\epsilon_c}(t)$ at the cage scale, $\epsilon=\epsilon_c$, for four different T.

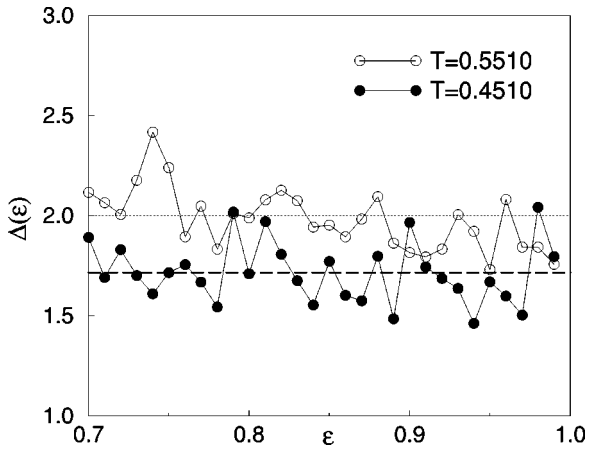

FIG. 11. Apparent fractal dimension $\Delta(\epsilon)$ of particle displacements in regime III. From Fig. 8, the highest and lowest simulation temperatures $T=0.5510$ and 0.4510 are shown for $0.7<\epsilon<1.0$.

A transition to intermittent particle motion at the glass transition was also suggested by Douglas and Hubbard [37]. Our observations are consistent with the growth of intermittency of particle motion as T_c is approached, but we cannot confirm theoretical predictions of a dynamical transition in the degree of intermittancy until lower temperatures are examined. An accurate test of these predictions will require carefully equilibrated data below T_c, beyond the temperature range of the simulations analyzed here. We point out that, in the present system, the scale at which this intermittency occurs is substantially *smaller* than one interparticle spacing, and instead pertains to motion at the scale of the cage size, ϵ_c.

C. Regime of persistent particle motion

Previous work has shown that particle motion becomes increasingly collective in this supercooled liquid, and that an important mode of motion at the scale of the interparticle distance involves the stringlike collective motion of particles. A visualization of this process [50] suggested to us that this process becomes increasingly ''coherent'' or ''jumplike'' at lower temperatures, and this tendency toward ''coherent jumping'' has been noticed in a number of other physical systems (melting of hard disks [51], hexatic liquids [52] and ordering plasmas [53]). In this subsection we utilize $S(\epsilon)$ to further quantify this effect.

Regimes I and II were defined by characteristic spatial scales at which changes occur in the first-passage time distributions. However, the long run times of the simulations analyzed here necessitated the storing of configurations on a logarithmic, rather than linear, time scale, for all but the coldest simulation [3]. As a consequence, first-passage time distributions cannot be obtained over a continuous range of ϵ for large ϵ. In the absence of complete information, we roughly identify regime III by the tendency for the non-Gaussian parameter $\alpha(t)$ to decrease (see Fig. 4). In Fig. 11 we show the apparent fractal dimension $\Delta(\epsilon)$ in regime III for the highest and lowest temperatures. (The results for all T are shown over an extended scale in Fig. 8). Notice that persistent particle motion $[\Delta(\epsilon)<2]$ develops for $\epsilon>0.6$ in Fig. 8 (although Δ remains near 2 at the highest temperatures) and consequently we show $\Delta(\epsilon)$ for the range $0.7<\epsilon<1.0$ in Fig. 11. The value of ϵ at which $\Delta(\epsilon)=2$ provides a more precise estimate for the beginning of regime III. Although the data are noisy, we find that $\Delta(\epsilon)\approx 2$ for high T within numerical error, and is nearly independent of ϵ. Particle displacement at high temperature is then reasonably approximated by Brownian motion on these spatial scales. However, a substantially smaller average value of $\Delta(\epsilon)\approx 1.7$ (dashed line in Fig. 11) is found for the lowest T. Thus, we find the particle motion becomes increasingly persistent on cooling.

Why is persistent motion not observed in the mean square displacement? The tendency for persistent particle motion is not apparent in $\langle r^2(t)\rangle$ shown in Fig. 2 or in the inset of Fig. 4 because, when averaging over the squared displacements, the contribution of the few particles that are at any given time moving persistently is ''washed out.'' However, these particles give a large contribution to the mean first-passage time, so that this quantity is therefore a more sensitive indictor of persistent particle motion.

We can obtain insight into the emergence of persistent particle motion in our cooled liquid from idealized models of Brownian motion subject to potential fluctuations. If the potential fluctuations are quenched, there is a tendency toward particle localization [54], but the occurrence of fluctuations in the potential in both space and time can lead to persistent particle motion. In particular, if the fluctuations are δ correlated in both space and time, then the exponent Δ equals 3/2 [55]. The effects observed in Ref. [55] are qualitatively consistent with our understanding of the origin of correlated motion. At short times, the existence of relatively immobile particles leads to a randomly fluctuating field ''felt'' by those particles free to move at a given point in time. This spatially fluctuating field is responsible for the particle caging or localization on time scales short compared to the decorrelation time τ_α of the ''structural fluctuations'' (associated with the relatively immobile particles). At longer times, the formerly immobile particles become mobile and the potential field fluctuates in time, leading to an enhancement in the particle displacement. At still longer times, thermal fluctuations (and associated additive noise) restore equilibrium and particle displacement ultimately becomes diffusive.

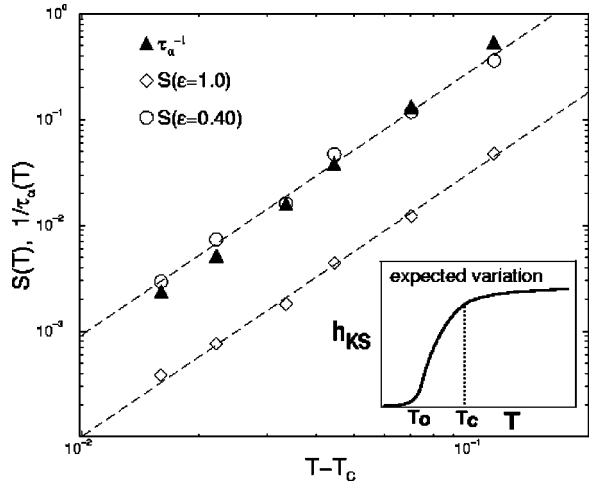

FIG. 12. Dynamic entropy $S(T,\epsilon)$ at the scale of one interparticle separation, $\epsilon=1$, vs $T-T_c$, with $T_c=0.435$. Diamonds refer to the simulation data for $S(\epsilon=1)$, and the dashed lines refer to the power law, $S(T)\sim(T-T_c)^{2.5}$. We also observe this scaling for $S(\epsilon=0.4)$ (circles). The inverse of the structural relaxation $1/\tau_\alpha$ (triangles) follows a power law $1/\tau_\alpha\sim(T-T_c)^{2.8}$. Inset: Schematic indication of expected temperature variation of dynamic entropy h_{KS} at small scales. Note that the extrapolated ergodic-nonergodic transition in the $\epsilon\to0$ limit is indicated to occur at a temperature $T_0<T_c$.

Finally, we point out that particle motion can be persistent even in the absence of a secondary (so-called ''hopping'') peak in $G_s(r,t)$. Instead, persistent particle motion contributes to a long tail in $G_s(r,t)$ in the temperature range of the present system [3,4]. This long tail develops into a secondary peak at lower T [56], indicating the increased contribution of collective particle motion to transport below T_c.

D. Large scale particle displacement

Particle displacement in a liquid at large scales is described by Brownian motion so that $S(\epsilon)$ should scale asymptotically as ϵ^2 for large ϵ, regardless of temperature. It is apparent in Fig. 2 that the data in the asymptotic diffusive regime are limited, especially at lower temperatures. Previous work has shown that there is a tendency for ''mobile'' particles, which dominate transport in cooled liquids near T_c, to move an interparticle distance during the time in which they are mobile [2–5]. This happens because the particles tend to move between local minima in the potential surface describing the interparticle interaction [56,57]. This feature is especially apparent in the stringlike particle motion noted before, where it has been observed that the strings ''disintegrate'' once an interparticle displacement has been achieved [2]. Thus one interparticle distance is taken to be the minimal scale of the large scale particle displacement regime (regime IV).

In the previous discussion, we have established that $S(\epsilon)$ is insensitive to temperature for small ϵ over the temperature range investigated. This insensitivity accords with the expected variation of dynamic entropy h_{KS}. At higher T we expect the dynamic entropy to saturate, while a decrease should accompany the more restricted particle motion at lower T [25]. A variation similar to that shown in the inset of Fig. 12 has been established for the ordering of the XY model [24]. The investigation of the anticipated ergodic-nonergodic transition and its possible relation to a vanishing of h_{KS} requires the calculation of the full Lyapunov spectrum, which is currently prohibitive for a system of the present size. However, we can investigate $S(\epsilon)$ at a larger scale on the order of an interparticle spacing. This should be interesting because of the strong T dependence in $S(\epsilon)$ at this length scale noted above (see Fig. 3).

In Fig. 12 we examine the T dependence of $S(T;\epsilon)$ at the scale of one interparticle separation $\epsilon=1$. We observe that $S(T;\epsilon=1)$ obeys a power law to a good approximation over the temperature range investigated, and that $S(T;\epsilon=1)$ seems to extrapolate to zero at the mode-coupling temperature $T_c=0.435$. As shown in Fig. 12, a reasonable fit to the data is obtained with the relation

$$S(\epsilon=1)\sim(T-T_c)^{2.5},\quad T_c=0.435. \tag{3.9}$$

The scaling of $S(\tau;\epsilon=1)$ is compared in Fig. 12 to the structural relaxation time τ_α describing the decay of the intermediate scattering function. Although the scaling of the two quantities is qualitatively similar, the best fit exponent for τ_α has the somewhat larger value of -2.8.

The power-law scaling of $S(\epsilon=1)$ with temperature is not obvious since if the particle displacement were exactly described by Brownian motion, then $\tau(\epsilon)$ would scale in inverse proportion to the diffusion coefficient. A determination of the diffusion coefficient for A particles is obtained by a simple least-squares fit (not shown) of the long time data to the function $\langle r^2(t)\rangle=A+6Dt$. This fitting gives

$$D\sim(T-T_c)^{2.1}. \tag{3.10}$$

A more refined estimate by Kob and Anderson [39] on a smaller (1000 particles) system gave an exponent 2.0 for the A particles. The diffusion data thus scales with a fractional power of the structural relaxation time,

$$D\sim\tau_\alpha^{-(2.1/2.8)}\simeq\tau_\alpha^{-0.75}, \tag{3.11}$$

over the temperature range investigated. Since evidence supports a common temperature scaling of τ_α and the fluid viscosity η [58], the observation implied by Eq. (3.11) is consistent with the breakdown of the Stokes-Einstein relation in real and simulated supercooled liquids [59–61]. We therefore conclude that $S(\epsilon=1)$ scales neither exactly like the inverse structural relaxation time $1/\tau_\alpha$ nor like the diffusion coefficient D. Other characteristic times exist for this liquid. It has recently been reported for the same simulations investigated here that the time scale on which particle displacements are most correlated scales as a power law with $(T-0.435)$, with an exponent $\gamma=2.3\pm0.2$ [7]. This exponent notably agrees within numerical error with the exponent in Eq. (3.9). We further note that the time t^* at which $\alpha(t)$ is a maximum (see Fig. 4) appears to diverge as $T\to T_c$ with an exponent 1.7 [3].

Since the temperature dependence of $S(\epsilon)$ is largest in Fig. 3 for $\epsilon=1$ and very small for $\epsilon\to0$, it is natural to consider the temperature dependence of $S(\epsilon)$ for many fixed ϵ to determine how this crossover occurs. In Fig. 13 we see that the scaling $S(T)\propto(T-T_c)^{2.5}$ holds for ϵ greater than the

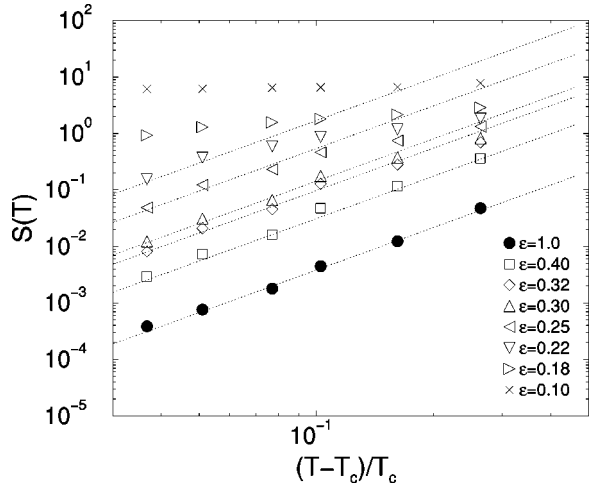

FIG. 13. Dynamic entropy $S(T,\epsilon)$ vs $T-T_c$, calculated at fixed values of ϵ. Dotted lines denote the power law, $S(T)\sim(T-T_c)^{2.5}$.

cage size ϵ_c and sufficiently small reduced temperature. We also find that for any temperature, the scaling fails for $\epsilon<\epsilon_c$. This provides another method for determining the cage size.

IV. CONCLUSION

We have studied the length-scale and temperature dependence of the dynamic entropy $S(\epsilon)$ in a molecular dynamics simulation of a model supercooled binary Lennard-Jones liquid. The simulations were performed above both the glass transition temperature and the mode-coupling critical temperature T_c and correspond to equilibrated liquid states [3].

$S(\epsilon)$ as estimated by the MFPT provides a tool for identifying characteristic length and time scales of the dynamics of liquids and provides a means for quantifying the degree of correlated motion occurring in supercooled liquids. At very small ϵ we observe a decorrelation of particle velocity and an $S(\epsilon)$ which is insensitive to temperature and ϵ variation. A decorrelation time associated with an average interparticle collision time is identified. At intermediate values of ϵ we observe a sharp drop in $S(\epsilon)$ with increasing ϵ, indicating that the path motion is more ''stochastic'' at these length scales. $S(\epsilon)$ is found to have a strong temperature dependence as well in this regime. The logarithmic derivative $\Delta \equiv d\ln\pi/d\ln\epsilon$ becomes a maximum at a characteristic ϵ value that is identified with the particle ''cage'' size ϵ_c, since particle localization is maximal at this point. The scaling of $S(\epsilon)$ with temperature at fixed ϵ gives an independent confirmation of our estimation of ϵ_c because it exhibits a qualitatively different dependence on temperature for $\epsilon>\epsilon_c$ and $\epsilon<\epsilon_c$. The localization parameter $\Lambda\equiv\Delta(\epsilon_c)$ increases and the cage size ϵ_c decreases as the liquid is cooled. The distribution functions for the first-passage time at the scale of the cage size, $P_{\epsilon_c}(t)$, in the coldest runs exhibit a long power-law tail, consistent with suggestions that there is growing intermittency in the particle displacements in glass-forming liquids [36,37]. This feature requires further study in cooler liquids to check the predictions of these models. At still larger scales (still less than one interparticle separation) we observe persistent motion which follows the transient particle ''caging.'' $S(\epsilon)$ obeys a power law $S(\epsilon)\sim\epsilon^{-1/\nu}$ for ϵ in the range (0.7,1) where the apparent fractal dimension of the particle trajectories $\Delta(\epsilon)=1/\nu$ ranges from ≈ 2 to ≈ 1.7 as the temperature is lowered. Thus, we observe a tendency for the particle motion to acquire a persistent character relative to Brownian motion as it is cooled. This is consistent with the previous observation of correlated stringlike motion in this liquid [2] and gives a single particle displacement perspective on this phenomenon.

General arguments suggest that the dynamic entropy at microscopic scales decreases at low temperatures, but a slower variation should be obtained at higher temperatures, as in the present molecular dynamics calculation (see Fig. 2). The situation is not so clear for the first-passage time dynamic entropy $S(\epsilon)$ at the scale of one interparticle separation $\epsilon=1$. In this case $S(\epsilon=1)$ is inverse to the ''average interparticle exchange time [62],'' $\tau(\epsilon=1)$. We find that $S(\epsilon)$ vanishes as a power law, $S(\epsilon=1)\propto(T-T_c)^{2.5}$, when the mode-coupling temperature T_c is approached from above. Thus, the cooled liquid has the appearance of approaching an ergodic to nonergodic transition as $T\rightarrow T_c$, when viewed at the scale $\epsilon=1$. This is consistent with the predictions of mode-coupling theory.

The first-passage time can also be utilized to obtain information about the spatial dependence of mobility fluctuations in cooled liquids. Perera and Harrowell [63], for example, examined the position dependence of τ at the scale of one interparticle spacing in a two-dimensional soft-sphere supercooled liquid, and found a tendency for particles of relatively high and low ''mobility'' (i.e., small and large τ, respectively) to cluster as T is lowered. A detailed study of spatial correlations of first-passage times in the present system will be presented elsewhere [64].

Future work should examine our approximate expression for $S(\epsilon)$ in the $\epsilon\rightarrow 0$ limit through independent calculation of the Kolmogorov-Sinai dynamic entropy, $S(\epsilon\rightarrow 0)\equiv h_{\mathrm{KS}}$. The temperature dependence of h_{KS} in cooler liquids ($T<T_c$) should be examined to determine if there is a tendency for the ''bare'' dynamic entropy to vanish at a lower glass transition temperature (see the inset of Fig. 12). Recent work has established a phenomenological relation between dynamic entropy h_{KS} and the equilibrium entropy in simulations of model liquids at relatively elevated temperatures [46]. A decrease in h_{KS} at lower T should be accompanied by the development of collective motion at short times. Such motion was reported in Ref. [49]. We expect this change in the short time dynamics to be relevant for interpreting the boson peak phenomenon in cooled liquids [65]. Simulations have already shown that the fraction of unstable modes f_u in a cooled liquid decreases in parallel with h_{KS} [25], and the vanishing of f_u has been identified with the temperature where the diffusion coefficient D vanishes [66,67].

Finally, we note that the calculation for $S(\epsilon)$ can be extended to other dynamical variables associated with other transport properties (viscosity, thermal conductivity, etc.), and these calculations should provide useful estimates of other characteristic space and time scale in cooled liquids [68]. We emphasize that although the definition of $S(\epsilon)$ is motivated by dynamical systems theory concepts, this quantity defines an independently interesting measure of correlated motion in liquids that does not rely on the approximation relating $S(\epsilon)$ to $h(\epsilon)$.

[1] W. Götze and L. Sjögren, Rep. Prog. Phys. **55**, 241 (1992); W. Götze, in *Liquids, Freezing and the Glass Transition*, edited by J. P. Hansen, D. Levesque, and J. Zinn-Justin, Les Houches Section LI (North-Holland, Amsterdam, 1991); U. Bengtzelius, W. Götze, and A. Sjölander, J. Phys. C **17**, 5915 (1984); E. Leutheusser, Phys. Rev. A **29**, 2765 (1984).

[2] C. Donati, J. F. Douglas, W. Kob, S. J. Plimpton, P. H. Poole and S. C. Glotzer, Phys. Rev. Lett. **80**, 2338 (1998).

[3] C. Donati, S. C. Glotzer, P. H. Poole, W. Kob, and S. J. Plimpton, Phys. Rev. E **60**, 3107 (1999).

[4] W. Kob, C. Donati, S. J. Plimpton, P. H. Poole, and S. C. Glotzer, Phys. Rev. Lett. **79**, 2827 (1997).

[5] S. C. Glotzer and C. Donati, J. Phys.: Condens. Matter **11**, A285 (1999).

[6] S. C. Glotzer, C. Donati, and P. H. Poole, in *Computer Simulation Studies in Condensed-Matter Physics XI*, edited by D. P. Landau *et al.* (Springer-Verlag, Berlin, 1999).

[7] C. Donati, S. C. Glotzer, and P. H. Poole, Phys. Rev. Lett. **82**, 5064 (1999).

[8] C. Bennemann, C. Donati, J. Baschnagel, and S. C. Glotzer, Nature **399**, 246 (1999).

[9] G. Adam and J. H. Gibbs, J. Chem. Phys. **43**, 139 (1965).

[10] J. H. Gibbs and E. A. DiMarzio, J. Chem. Phys. **28**, 373 (1958).

[11] D. Thirumalai, R. D. Mountain, and T. Kirkpatrick, Phys. Rev. A **39**, 3563 (1989); in this reference the authors introduced an energy metric to quantify the time scale over which effective ergodicity is achieved in simulations.

[12] N. S. Krylov, *Works on the Foundations of Statistical Mechanic* (Princeton University Press, Princeton, 1979); Nature **153**, 709 (1944); see also Ch. Delago and H. A. Posch, Phys. Rev. E **55**, R9 (1997).

[13] A. N. Kolmogorov, Dokl. Acad. Sci. USSR **124**, 754 (1959); Y. G. Sinai, *ibid.* **124**, 768 (1959).

[14] P. Gaspard and X.-J. Wang, Phys. Rep. **235**, 291 (1993), and references therein.

[15] P. Gaspard, Adv. Chem. Phys. **99**, 369 (1997).

[16] G. M. Zavslavsky, Phys. Rep. **80**, 157 (1981).

[17] J. Lebowitz and O. Penrose, Phys. Today **26** (2), 23 (1973).

[18] C. E. Shannon, Bell Syst. Tech. J. **27**, 379 (1948); **27**, 623 (1948); C. E. Shannon and W. Weaver, *Mathematical Theory of Communication* (University of Illinois Press, Urbana, 1949).

[19] Ya. B. Pessin, Russ. Math. Surv. **32**, 55 (1977); J. P. Eckman and D. Ruelle, Rev. Mod. Phys. **57**, 617 (1985).

[20] R. Livi, A. Politi, and S. Ruffo, J. Phys. A **19**, 2033 (1986).

[21] J. R. Dorfman, Phys. Rep. **301**, 151 (1998).

[22] G. J. Chaitin, Sci. Am. **232**, 47 (1975); A. N. Kolmogorov, Russ. Math. Surv. **38**, 29 (1983).

[23] P. W. Cleary, J. Math. Phys. **30**, 689 (1989).

[24] P. Butera and G. Caravati, Phys. Rev. A **36**, 962 (1987); The maximum Lyapunov exponent is aproximately proportional to h_{KS} [14,20].

[25] Ch. Dellago and H. Posch, Physica A **230**, 364 (1996).

[26] L. Caiani, L. Casetti, C. Clementi, and M. Pettini, Phys. Rev. Lett. **79**, 4361 (1997).

[27] D. J. Wales and R. S. Berry, J. Phys. B **24**, L351 (1991); R. J. Hinde and R. S. Berry, J. Chem. Phys. **99**, 2942 (1993).

[28] T. Berger, IEEE Trans. Inf. Theory **IT-16**, 134 (1970).

[29] The existence of a finite, positive h_{KS} is often taken as a defining characteristic of ''chaos'' in a dynamical system, but this definition excludes Brownian motion, the prototypical model of chaotic motion in molecular physics [N. Wiener, Am. J. Math. **60**, 897 (1938)] since $h_{\mathrm{KS}} \to \infty$ [14] for Brownian motion. The extension of dynamic entropy to the scale dependent quantity $h(\epsilon)$ resolves this unsatisfactory situation.

[30] B. B. Mandelbrodt, *The Fractal Geometry of Nature* (Freeman, San Francisco, 1977).

[31] H. P. McKean, Jr., Duke Math. J. **22**, 229 (1955); S. J. Taylor, Proc. Cambridge Philos. Soc. **49**, 31 (1953).

[32] R. K. Getoor, Trans. Am. Math. Soc. **101**, 75 (1961).

[33] P. Gaspard, M. E. Briggs, M. K. Francis, J. V. Sengers, R. W. Gammon, J. R. Dorfman, and R. V. Calabrese, Nature **384**, 865 (1998).

[34] The diffusion coefficient of the two-dimensional Lorentz gas has been calculated from a consideration of the escape rate of a diffusing tracer (point particle) scattered by its local environment of impenetrable disks [P. Gaspard and G. Nicolis, Phys. Rev. Lett. **65**, 1693 (1990)]. This work has stimulated the investigation of local escape rates as a measure of particle mobilities in cooled liquids [B. Reardon and J. Kieffer (unpublished)].

[35] Previous work identifying instances of stringlike collective motion in simulations of supercooled liquids includes J. L. Barrat, J. N. Roux, and J. P. Hansen, Chem. Phys. **149**, 197 (1990); H. Miyagawa, Y. Hiwatari, B. Bernu, and J. P. Hansen, J. Chem. Phys. **86**, 3879 (1988); G. Wahnström, Phys. Rev. A **44**, 3752 (1991).

[36] T. Odagaki, Phys. Rev. Lett. **75**, 3701 (1995). See also T. Odagaki and Y. Hiwatari, Phys. Rev. A **41**, 929 (1990); J. Phys.: Condens. Matter **3**, 5191 (1991).

[37] J. F. Douglas and J. B. Hubbard, Macromolecules **24**, 3163 (1991); J. F. Douglas, Comput. Mater. Sci. **4**, 292 (1995).

[38] The Lennard-Jones interaction parameters $\epsilon_{\alpha,\beta}$ and $\sigma_{\alpha,\beta}$ are given by $\epsilon_{AA}=1.0$, $\epsilon_{AB}=1.5$, $\epsilon_{BB}=0.5$, $\sigma_{AA}=1.0$, $\sigma_{AB}=0.8$, and $\sigma_{BB}=0.88$. Lengths are defined in units of σ_{AA}, temperature T in units of ϵ_{AA}/k_B, and time t in units of $\sqrt{\sigma_{AA}^2 m/\epsilon_{AA}}$.

[39] W. Kob and H. C. Andersen, Phys. Rev. Lett. **73**, 1376 (1994); Phys. Rev. E **51**, 4626 (1995); **52**, 4134 (1995).

[40] Recall that for this same system simulated along a different path, the same value of T_c was found from an analysis of the minority (B) particles only [39].

[41] C. A. Angell, Science **297**, 1945 (1995).

[42] M. H. Lee, Phys. Rev. Lett. **51**, 1227 (1983).

[43] Equipartition of energy implies that the average square velocity v_0^2 in Eq. (3.6) is proportional to kT/m, where m is the particle mass. The mass in this expression can become renormalized by backflow after a short time (time for a sound wave to propagate an interparticle distance, approximately 10^{-14} s in liquid argon) in a compressible liquid [R. Zwanzig and M. Bixon, J. Fluid Mech. **69**, 21 (1975)]. Collective effects can thus develop at very short times.

[44] D. A. McQuarrie, *Statistical Mechanics* (Harper and Row, New York, 1976).

[45] Z. Ciesielski and S. J. Taylor, Trans. Am. Math. Soc. **103**, 434 (1962).

[46] M. Dzugutov, E. Aurell, and A. Vulpiani, Phys. Rev. Lett. **81**, 1762 (1998); see also V. Latora and M. Baranger, Phys. Rev. Lett. **82**, 520 (1999).

[47] H. A. Posch and W. G. Hoover, Phys. Rev. A **38**, 473 (1988); **39**, 2175 (1989); D. G. Evans, E. G. D. Cohen, and G. P. Morriss, *ibid.* **42**, 5990 (1990); S. D. Stoddard and J. Ford,

ibid. **8**, 1504 (1973); S. Sastry, Phys. Rev. Lett. **76**, 3738 (1996).
[48] B. Doliwa and A. Heuer, Phys. Rev. Lett. **80**, 4915 (1998).
[49] Y. Hiwatari and T. Muranaka, J. Non-Cryst. Solids **235–237**, 19 (1998).
[50] See http://www.ctcms.nist.gov/donati/movie.html.
[51] B. J. Alder, W. G. Hoover, and T. E. Wainwright, Phys. Rev. Lett. **11**, 241 (1963); B. J. Alder, D. M. Ceperley, and E. L. Pollack, Int. J. Quantum Chem., Symp. **16**, 40 (1982).
[52] C. A. Murray and R. A. Wenk, Phys. Rev. Lett. **62**, 1643 (1989); C. A. Murray, D. H. van Winkle, and R. A. Wenk, Phase Transit. **21**, 93 (1990); J. Q. Broughton, G. H. Gilmer, and J. D. Weeks, Phys. Rev. B **25**, 4651 (1982).
[53] Ph. Choquard and J. Clerouin, Phys. Rev. Lett. **50**, 2086 (1983).
[54] P. Grassberger and I. Procaccia, J. Chem. Phys. **77**, 6281 (1982); D. Wu, K. Hui, and D. Chandler, *ibid.* **96**, 835 (1992); A. Baumgartner and M. Muthukumar, *ibid.* **87**, 3082 (1987); J. F. Douglas, Macromolecules **21**, 3515 (1988).
[55] M. Kardar and Y. Zhang, Phys. Rev. Lett. **58**, 2087 (1987); M. Kardar, G. Parisi, and Y.-C. Zhang, Phys. Rev. Lett. **56**, 889 (1986).
[56] T. B. Schrøder and J. Dyre, J. Non-Cryst. Solids **235–237**, 331 (1998); T. B. Schrøder, S. Sastry, J. Dyre, and S. C. Glotzer, e-print cond-mat/9901271.
[57] R. A. LaViolette and F. H. Stillinger, J. Chem. Phys. **83**, 4079 (1985); J. Jellinek, T. L. Beck, and R. S. Berry, J. Chem. Phys. **84**, 2783 (1986); D. Wales, Science **271**, 925 (1996).
[58] R. Yamamoto and A. Onuki, Phys. Rev. Lett. **81**, 4915 (1998).
[59] Decoupling of transport properties in supercooled liquids has been investigated in, e.g., D. Ehlich and H. Sillescu, Macromolecules **23**, 1600 (1990); F. Fujara, B. Geil, H. Sillescu, and G. Fleischer, Z. Phys. B **88**, 195 (1992); I. Chang, F. Fujara, B. Geil, G. Heuberger, T. Mangel, and H. Sillescu, J. Non-Cryst. Solids **172–174**, 248 (1994); L. Andreozzi, A. Di Schino, M. Giordano, and D. Leporini, Europhys. Lett. **38**, 669 (1997); R. Yamamoto and A. Onuki, Phys. Rev. E **58**, 3515 (1998); M. T. Cicerone and M. D. Ediger, J. Chem. Phys. **104**, 7210 (1996); F. H. Stillinger and J. Hodgdon, Phys. Rev. E **50**, 2064 (1994); D. Thirumalai and R. D. Mountain, *ibid.* **47**, 479 (1993); A. Voronel, E. Veliyulin, V. Sh. Machavariani, A. Kisliuk, and D. Quitmann, Phys. Rev. Lett. **80**, 2630 (1998).
[60] It is important to note that D scales in inverse proportion to τ_α in mode-coupling theory, and that Eq. (3.11) suggests an important shortcoming of this model. Recent data for A-B dumbbell particles interacting with the same LJ parameters of the present calculation [S. Kammerer, W. Kob, and R. Shilling, Phys. Rev. E **56**, 5450 (1998)] exhibit a breakdown of the inverse scaling between D and the particle rotational relaxation time (which should scale as DNI/τ_α in mode-coupling theory).
[61] S. C. Glotzer, V. Novikov, and T. B. Schroeder, e-print cond-mat/9909113.
[62] J. Frenkel, *Kinetic Theory of Liquids* (Dover, New York, 1955).
[63] D. N. Perera and P. Harrowell, J. Non-Cryst. Solids **235–237**, 314 (1998); see also M. M. Hurley and P. Harrowell, Phys. Rev. E **52**, 1694 (1995).
[64] P. Allegrini and S. C. Glotzer (unpublished).
[65] D. Quitmann and M. Soltwisch, J. Non-Cryst. Solids **235–237**, 237 (1998); V. N. Novikov, Phys. Rev. B **55**, R14 685 (1997); J.-B. Suck, H. Rudin, H.-J. Güntherodt, and H. Beck, Phys. Rev. Lett. **50**, 49 (1983).
[66] G. Seeley and T. Keyes, J. Chem. Phys. **91**, 5581 (1989); P. Madden, T. Keyes, and G. Seeley, *ibid.* **94**, 6762 (1991). Recent work has shown that the fraction of unstable shoulder modes for the present LJ model tends to vanish as $T \rightarrow T_c$ [C. Donati *et al.* (unpublished)].
[67] F. Sciortino and P. Tartaglia, Phys. Rev. Lett. **78**, 2385 (1997).
[68] J. R. Dorfman and P. Gaspard, Phys. Rev. E **51**, 28 (1995); B. J. Alder, D. M. Gass, and T. E. Wainwright, J. Chem. Phys. **53**, 3813 (1970); E. Helfand, Phys. Rev. **119**, 1 (1960).